Master's Thesis
석사 학위논문

A Real-time Surface Registration-based Electrode Guidance System

Chanho Song (송 찬 호 宋 燦 豪)

Department of Robotics Engineering

로봇공학전공

DGIST

2017

Master's Thesis
석사 학위논문

A Real-time Surface Registration-based Electrode Guidance System

Chanho Song (송 찬 호 宋 燦 豪)

Department of Robotics Engineering

로봇공학전공

DGIST

2017

A Real-time Surface Registration-based Electrode Guidance System

Advisor : Professor Jaesung Hong
Co-advisor : Professor Sungbae Lee

by

Chanho Song
Department of Robotics Engineering
DGIST

A thesis submitted to the faculty of DGIST in partial fulfillment of the requirements for the degree of Master of Science in the Department of Robotics Engineering. The study was conducted in accordance with Code of Research Ethics[1]

. . 2017

Approved by

Professor Jaesung Hong (_____)
(Advisor)

Professor Sungbae Lee (_____)
(Co-Advisor)

[1] Declaration of Ethical Conduct in Research**:** I, as a graduate student of DGIST, hereby declare that I have not committed any acts that may damage the credibility of my research. These include, but are not limited to: falsification, thesis written by someone else, distortion of research findings or plagiarism. I affirm that my thesis contains honest conclusions based on my own careful research under the guidance of my thesis advisor.

A Real-time Surface Registration-based Electrode Guidance System

Chanho Song

Accepted in partial fulfillment of the requirements for the degree of Master of Science.

11. 29. 2016

Head of Committee	Prof. Jaesung Hong	(인)
Committee Member	Prof. Sungbae Lee	(인)
Committee Member	Prof. Cheol Song	(인)

MS/RT
201523005

송 찬 호. Chanho Song. A Real-time Surface Registration-based Electrode Guidance System. Department of Robotics Engineering. 2017. 34p. Advisors Prof. Jaesung Hong, Prof. Co-Advisors Sungbae Lee.

ABSTRACT

Electroencephalography (EEG) has been frequently used to measure the neural activity in brain researches. In EEG based longitudinal study, repeatability of electrode positioning is important for the consistent EEG assessment over a long period of time. Conventional methods including the international 10-20 or its expanded systems have been adopted to provide a standardized electrode positioning. The methods use four principal anatomical landmarks including nasion, inion, left and right pre-auricular points as fiducial locations for electrode placement. However, the landmarks are manually identified via visual inspection or palpation, involving variations in locations of affixed electrodes and in turn alterations in measured EEG signals. In this study, we proposed an electrode guidance navigation based on markerless augmented reality visualization, which aims to enable the precise electrode placement in a cost-effective way. The presented system uses a RGB-D camera for scanning and registration of facial surface or electrodes and thereby visualizes reference and current electrode position in real time. The experimental results from the phantom study confirmed that the positioning precision of the proposed system was improved in comparison with that of the conventional 10-20 positioning system. We believe that the presented system would be a possible alternative to the conventional systems for precise electrode placement in longitudinal EEG studies.

Keywords: Electrode positioning, The international 10-20 system, Markerless augmented reality, Surface registration

Contents

List of contents

List of tables

List of figures

I. INTRODUCTION

1.1 Introduction of augmented reality-based surgical navigation

Recent advance of vision robotics, computer science, electronic engineering and medical imaging technologies have led to the development of augmented reality (AR) based surgical navigation. Unlike the surgeon relied on the medical information in the preoperative procedure in the past, the AR-based surgical navigation provides necessary medical information for the surgeon during surgery. Based on the AR, visualization of the target organ or surrounding risk factor allows the surgeon to operate the surgery with more accurate and abundant medical information.

For the implementation of the AR-based surgical navigation, the patient to image registration is required between the CT/MRI image, which including the medical information required during the operation, and actual patient. The patient to image registration is the process to derive the transformation from the CT/MRI image coordinate system to patient coordinate system. The representative methods for the registration are paired point registration and surface registration. The paired point registration is a method to derive the transformation using the set of paired points in each coordinate system. The surface registration derives the transformation based on the surface information in each coordinate system. When the patient to image registration is performed, the transformation between a medical image such as CT/MRI and marker indicating the patient can be known, and the AR-based surgical navigation can be implemented.

The development of AR-based surgical navigation makes it possible for the surgeons to operate safer and more accurate surgery. The use of surgical navigation system can also reduce the operation time of surgery, thereby minimizing the burden on the patient. The surgical navigation is used in various surgeries and also can be applied to other medical fields such as rehabilitation, image-guided therapy as well as surgery.

1.2 Electroencephalography and electrode positioning system

Electroencephalography (EEG) is a neuroimaging technique, which is frequently used to measure the neural activity in the brain. EEG is a method to measure the neural activity based on the electric potential on the scalp. In EEG-based studies, standardized positioning of electrode is one of the important issues to minimize the test-retest and inter-subject variability [1, 2]. In longitudinal studies, small positioning error on the scalp can lead a large changes of electric potentials in EEG data [1]. Thus, every session of measurement in EEG, the electrode should be placed on the same location with repeatability.

In general, EEG technician uses the international 10-20 system to locate the EEG electrode on the subject's head [3-6]. The 10-20 system is a method for the standardized EEG electrodes positioning, based on the four anatomical landmarks which are the inion, nasion, left and right pre-auricular points [6, 7]. For the electrode positioning, the 10-20 system requires manual identification of the landmarks. After the identification, the midline from nasion to inion and the central line from left preauricular point to the right preauricular point are measured. Based on the two reference line, anterior-posterior plane and central coronal plane are determined, and the

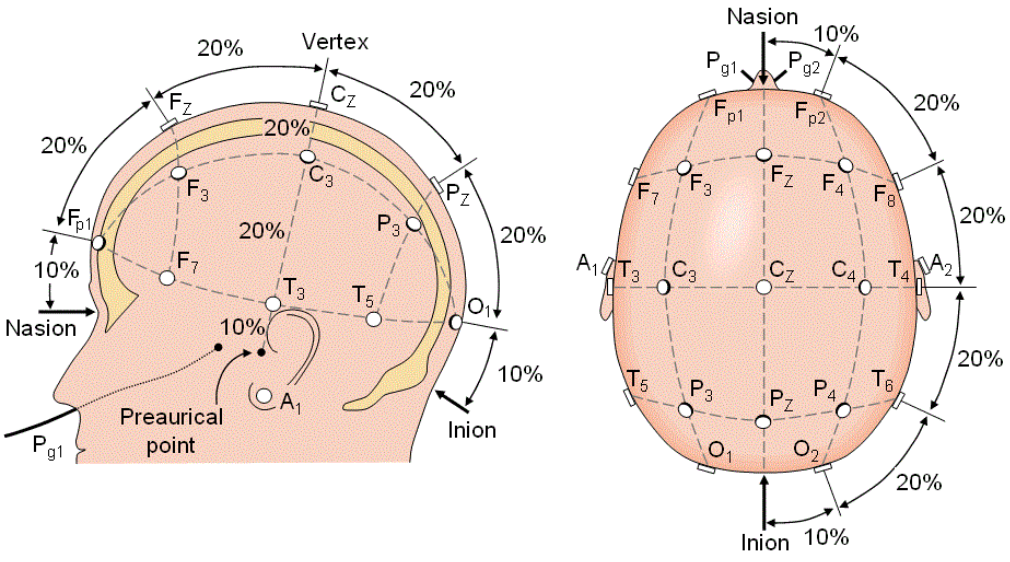

Figure 1.1 International 10-20 system.

electrodes are placed with 10% and 20% intervals [7]. The 10-20 system is a manual method which does not required specific equipment.

1.3 Conventional methods

Echallier and Perrin proposed a computer-assist electrode positioning system [8]. An ultrasonic digitizer was used to calculate the reference coordinate system based on the four anatomical landmarks. Then, the reference positions of the electrodes were saved with respect to the coordinate system using the digitizer. When repositioning the electrodes, their system showed the current position of each electrode with respect to saved reference electrode positions. For the electrode repositioning, procedure for digitizing the four anatomical landmarks were required as initial starting points.

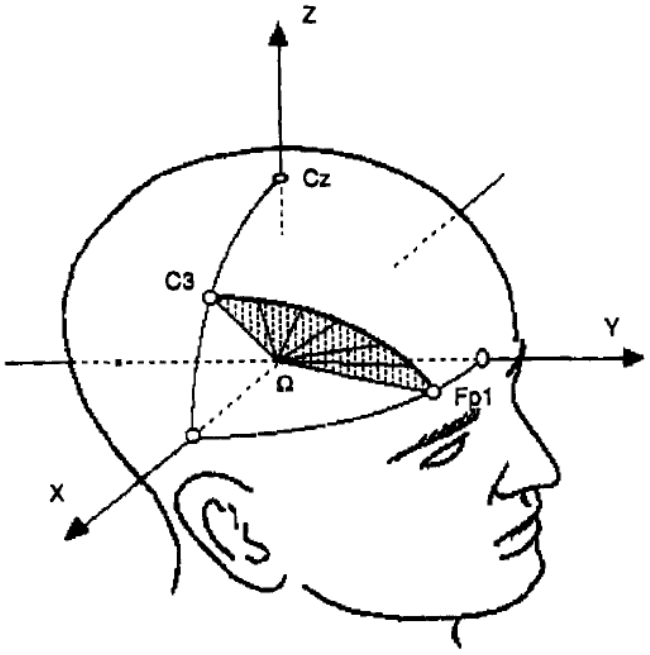

Figure 1.2 Reference coordinate system based on anatomical landmarks.

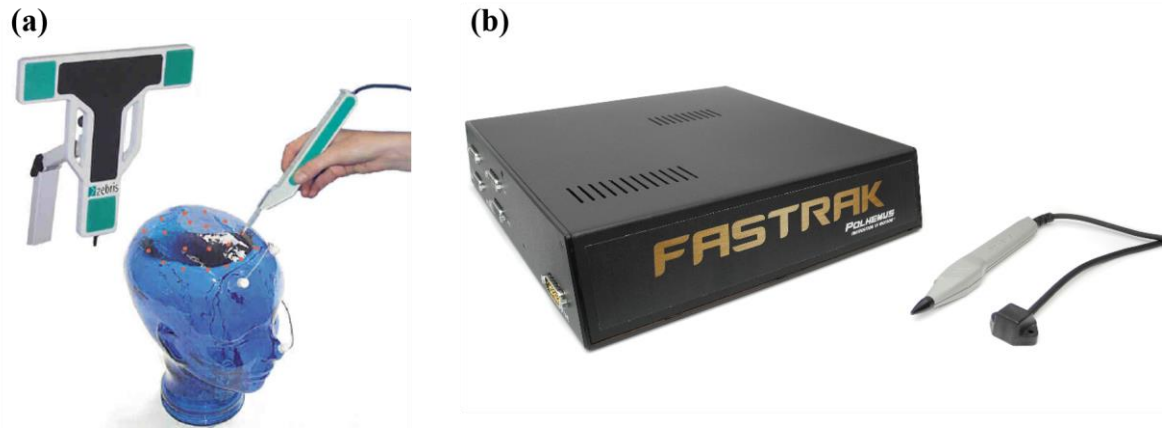

Figure 1.3 Commercial product of ultrasonic and electromagnetic digitizer**.** (a) Ultrasonic digitizer for determining EEG electrode positions. (b) Electromagnetic digitizer for localization of the EEG electrode and fNIRS optode.

Figure 1.3. shows the commercial product of ultrasonic digitizer (ELPOS, Zebris, Tuebingen, Germany) and electromagnetic digitizer (FASTRAK, Polhemus, Colchester, USA) for the electrode positioning and localization. The ELPOS system is a commercial product for accurate EEG electrode positioning. The electrode positioing method of the ELPOS system is very similar to that of the computer-assisted electrode placement system. The ELPOS system required manual digitization of human anatomical landmarks in the process of electrode positioning, and saved the each position of electrodes using digitizer. When repositioning, the user should compare each current electrode position with respect to saved reference positions. The FASTRAK system is a commercial product for localization of EEG electrode and fNIRS optode. The localization process of the FASTRAK system is also similar to that of the computer-assisted electrode placement system, and manual digitization process of human anatomical landmarks is required.

Commercial systems assure the high accuracy of the electrode positioning in terms of specifications. However, both ultrasonic and electromagnetic system are very expensive and sensitive to environment condition such as temperature, humidity and electric fields. Also, manual digitization of each individual position is time consuming task for both electrode and optode positioning [9].

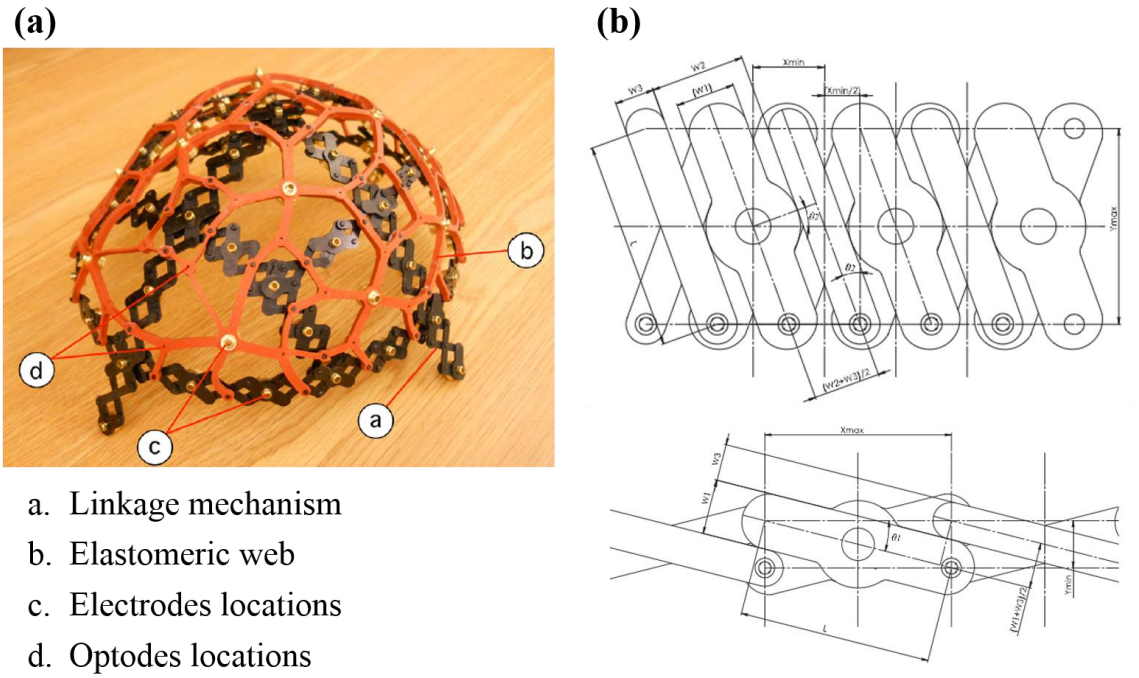

Figure 1.4 (a) Compliant head probe for EEG electrode and NIRS optode. (b) Linkage mechanism for fitting the desired head size.

Giacometti et al. developed a cap for standardized positioning available for both electroencephalography (EEG) and functional near-infrared spectroscopy (fNIRS), called "NIRS-EEG cap" [2]. The linkage mechanism was adopted for fitting the desired head size, and size of the cap's web was determined by statistical head model. In the literature, to test the repeatability of electrode position, the cap was placed using the 10-10 system that is an expanded system of the international 10-20 system. The performance of the cap was compared with that of commercial product (Advanced Neuro Technology, ANT B.V., Enschede, Netherlands), and showed less positioning error in the phantom study.

For the electrode positioning, the previous researches have approached in the various viewpoint. However, such systems have in common with conventional 10-20 system, which require the manual identification of the anatomical landmarks in the process of electrode positioning. The manual identification can yield non-negligible human error because of the ambiguity of the anatomical landmarks [6, 9].

1.4 Proposed method

In this study, we propose to use markerless augmented reality (AR) technique to enable precise electrode positioning without manual landmark identification. Studies have reported on AR techniques for medical applications, e.g. a markerless registration framework using three cameras and AR patterns for cranial AR system [10], similar one based on real-time image-to-patient surface registration for on-patient medical data visualization [11], or a visual SLAM-based AR system for on-patient AR visualization [12]. However, to our knowledge, this is the first study to deploy AR visualization technique for precise electrode positioning in EEG studies.

The proposed system makes use of facial surface information from a RGB-D camera as markers for surface registration. Following the registration, current and reference positions of electrodes are visualized in real time to enable electrode positioning without manual identification of 10-20 landmarks. A problem of heavy computational cost for real-time surface registration is addressed via a parallel pipeline enabling the surface registration to be processed independently of real-time scanning and visualization process. A phantom study was conducted to

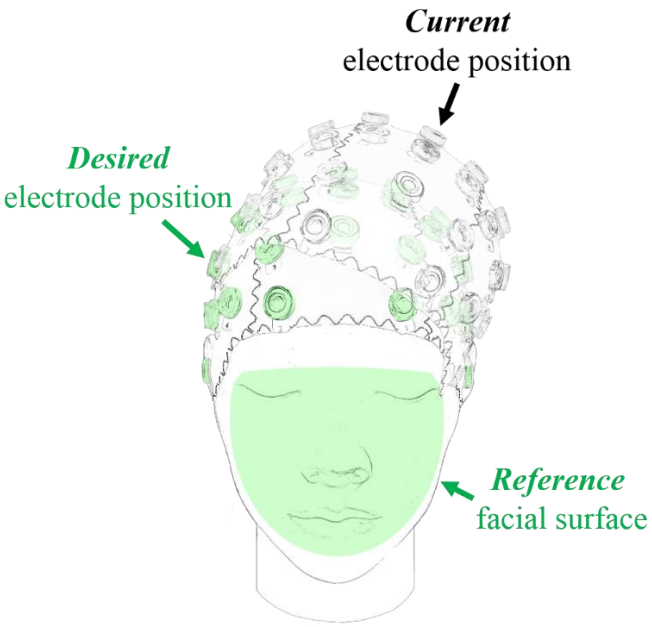

Figure 1.5 Augmented reality visualization for electrode guidance.

evaluate the effectiveness of the proposed system in terms of its electrode positioning precision, and the proposed system was compared with that of the conventional 10-20 system.

The rest of this paper is composed of as follow: The configuration of the proposed system are described in section 2.1. The procedure for the proposed electrode guidance method and its detail are described in section 2.2. The pipeline of real-time surface registration is described in section 2.3. The experimental preparation and methods for electrode positioning test are described in section 2.4. Section 3 presents the experimental result of electrode positioning test and performance of real-time surface registration. Finally, we discuss the proposed system and suggest the future works in section 4.

II. METHODS

2.1 Configuration of the system

2.1.1 System overview

The main purpose of the proposed system is to improve the repeatability of electrode positioning. For this, the proposed system provides AR visualization to an EEG technician.

The proposed system requires saved positions of electrodes. In the first electrode positioning on a patient head, positions of electrodes are saved and used as reference. When the technician relocates the electrodes to the patient head, current positions of electrodes are scanned by using a low-cost camera and visualized through a display by overlaying it on reference. Because AR visualization intuitively shows the current positions of electrodes with respect to reference, the technician can easily and exactly relocate the electrode on the previous position.

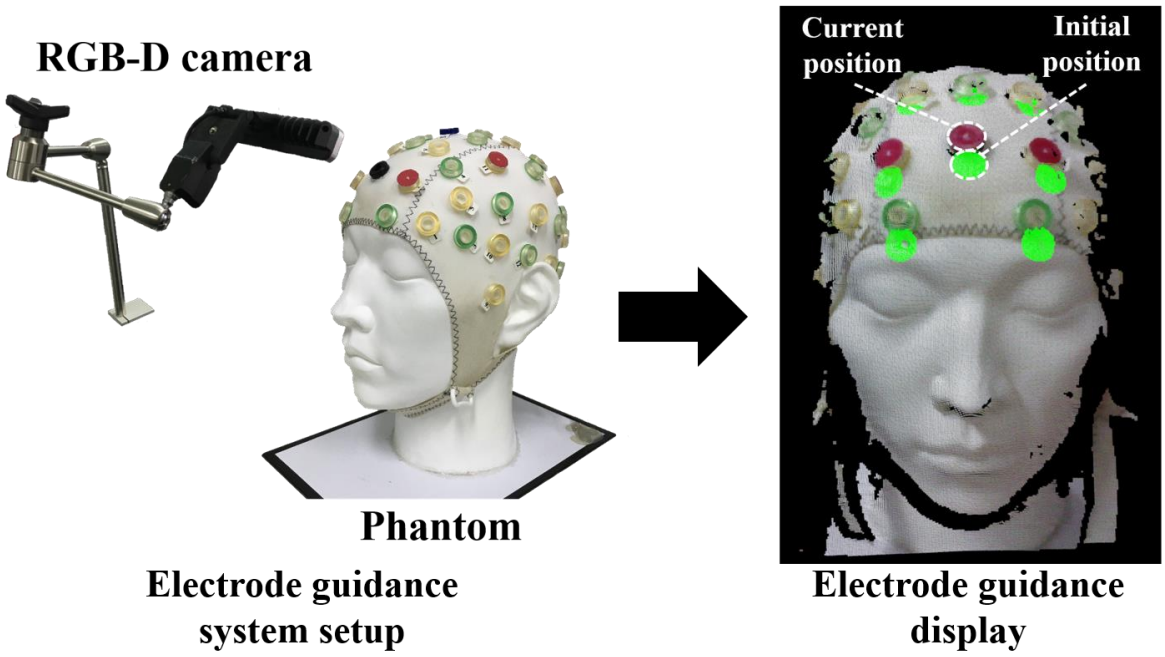

Figure 2.1 System setup for electrode guidance.

2.1.2 Development environment

The development environment of the proposed electrode guidance system is as follows; A RGB-D camera (Realsense f200, Intel, California, USA) was used to acquire the real-time scanning data as 3D point clouds following the image processing. By using the RGB-D camera, the depth and vision images are simultaneously obtained. A self-developed software was used to acquire, handle, and visualize 3D points from the RGB-D camera. In detail, a realsense camera software development toolkit was used for connection to the RGB-D camera and data acquisition of scanned 3D points, visualization toolkit (www.vtk.org) was used for visualization of processed data, and point cloud library [13] was used for handling the 3D points and developing an algorithm described later. In this study, the self-developed software was executed in a workstation equipped with an Intel Core i7 CPU, 32 GB RAM, and NVIDIA GeForce GTX 970 GPU.

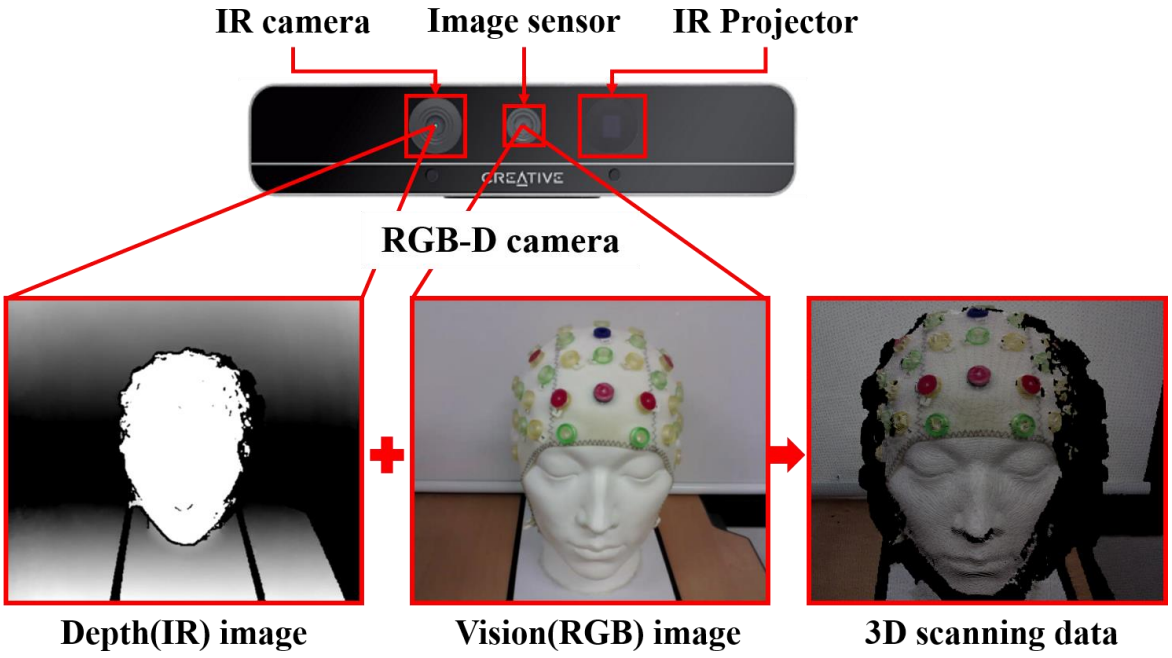

Figure 2.2 3D scanning of RGB-D camera.

2.2 Procedure for electrode guidance

The main purpose of the proposed system is to improve the repeatability of electrode positioning. For this, the proposed system provides AR visualization to an EEG technician. The proposed system requires saved positions of electrodes. In the first electrode positioning on a patient head, positions of electrodes are saved and used as reference. When the technician relocates the electrodes to the patient head, current positions of electrodes are scanned by using the RGB-D camera and visualized through a display by overlaying it on reference. Because that AR visualization shows current positions of electrodes with respect to reference, it is possible to relocate the current electrode on the previous reference position.

For the implementation of the electrode guidance, the system consists of two key steps: preparation step and navigation step as shown in Fig. 2.3. The preparation step is initial setup process to get the reference data. The reference data is composed of reference facial surface and reference electrode position. In the navigation step, the result of real-time surface registration between reference and current scanning data are visualized for electrode guidance. The details of preparation and navigation steps will be described in part 2.2.1 and 2.2.2, respectively.

2.2.1 Preparation step

In the preparation step, an electrode cap is initially positioned on the head of a subject using the 10-20 system. Then, the head of the subject including facial surface and electrode position are scanned using the RGB-D camera at one time. The facial surface and electrode position are separately segmented using an open source software (CloudCompare, France), and saved. The saved facial surface is used as input data for surface registration, and the saved electrode position is used as reference electrode position in the navigation step.

2.2.2 Navigation step

In the navigation step, the electrode is repositioned based on AR visualization technique which used in this study. To implement AR-based electrode guidance system, the 3D scanning and surface registration are performed in real time. In order to repositioning the electrode, the subject is scanned with the RGB-D camera. The scanned data is converted to 3D point cloud. Note that the 10-20 system is not required for repositioning the electrode.

The surface registration is performed between the reference facial surface acquired in preparation step and the real-time scanning data using the iterative closest point (ICP) algorithm. The ICP algorithm is a numerical method to calculate a transformation from the coordinate system of target surface to the coordinate system of source surface [14, 15]. Thus, it requires target and source input data. In this study, the reference facial surface is used for source data, and real-time scanning data is used for target data. As a result of surface registration, the

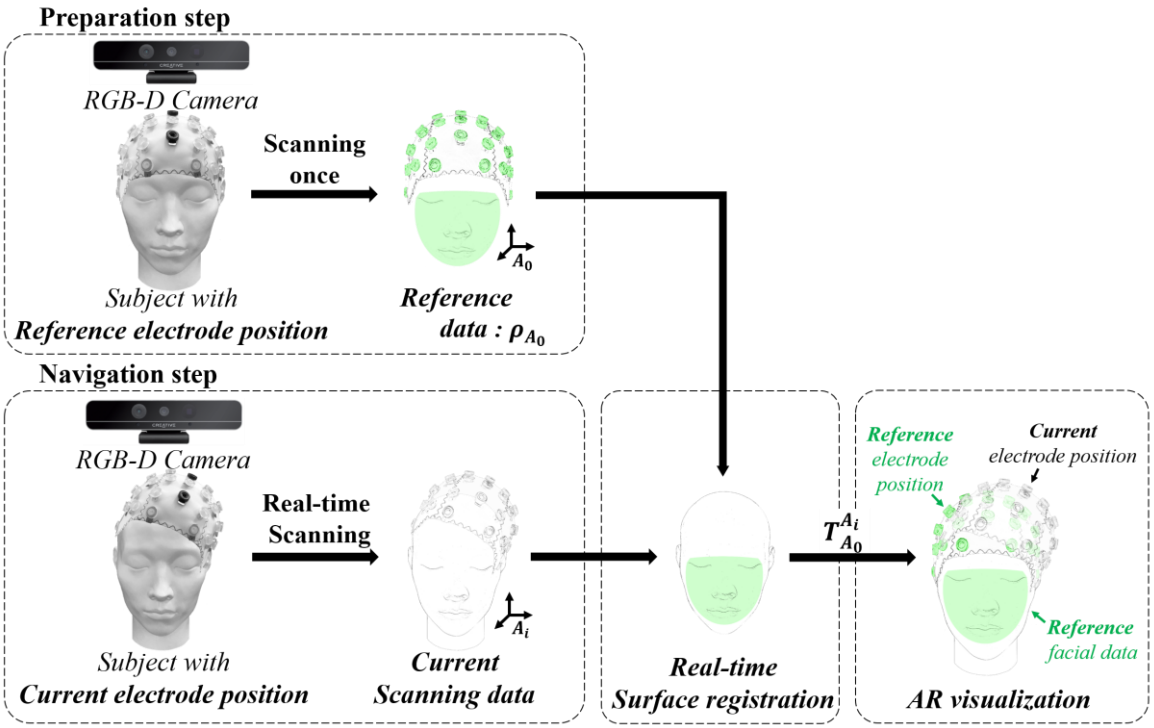

Figure 2.3 Procedure of electrode guidance system. The system is composed of two key steps: preparation step and navigation step. The preparation step is initial setup step to get the reference data. In the navigation step, the result of real-time surface registration between reference and current scanning data is visualized for electrode guidance.

transformation from current facial surface coordinate system to reference facial surface coordinate system is obtained. Therefore, during the real-time surface registration, the transformation is updated on the basis of current facial surface. By applying the transformation, the reference data is overlaid on the current facial surface. The details of real-time surface registration will be described in section 2.3.

In the navigation step, as a result of real-time scanning and registration, the reference data is overlaid on the current scanning data on the basis of the facial surface as shown in Fig. 2.4. The AR visualization shows both reference electrode position and current electrode position at the same time. Then, the EEG technician enable the current electrode to be placed on the reference position with high repeatability.

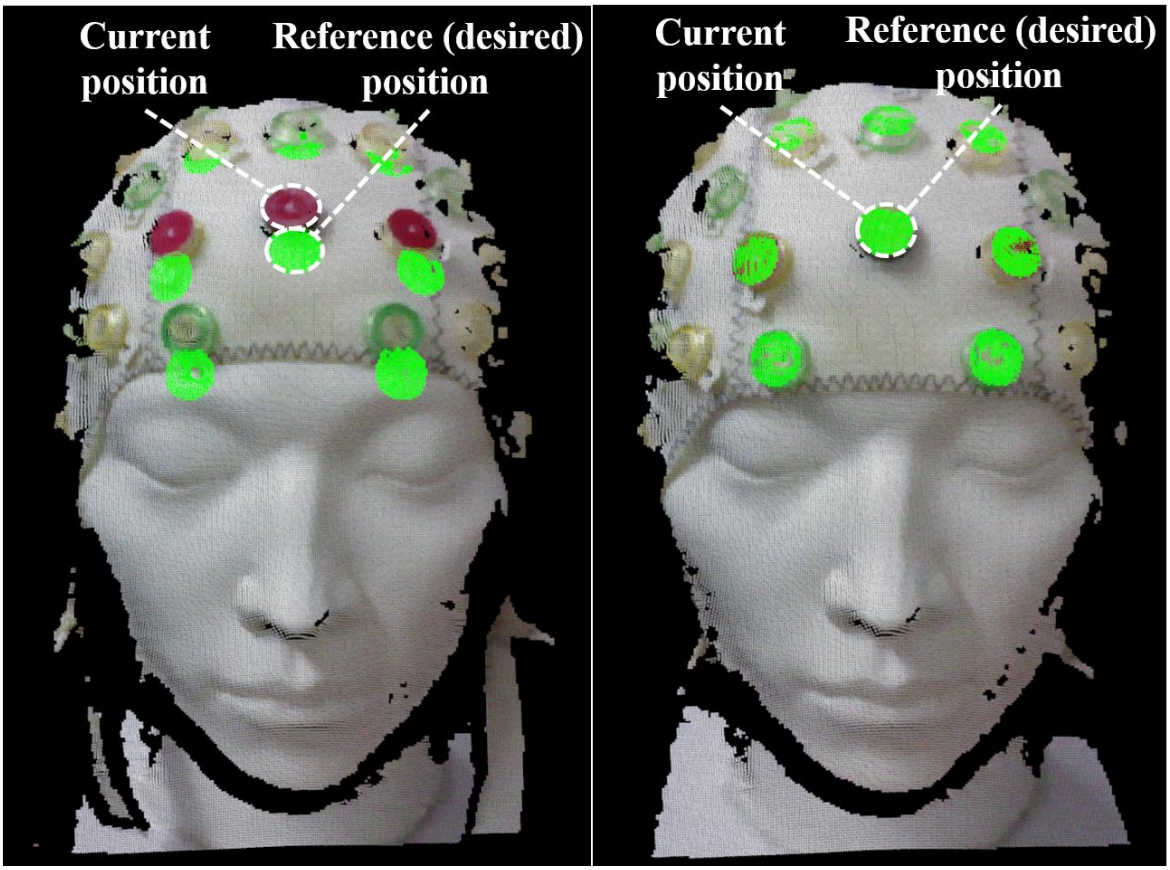

Figure 2.4 Electrode guidance display (left) during and (right) after the guidance.

2.3 Real-time surface registration

2.3.1 Iterative closest point algorithm

Surface registration is a method to calculate the transformation between two different coordinate system by using the three-dimensional surface information. A representative method of surface registration is the iterative closest point (ICP) algorithm. The ICP algorithm was first published by Besl and Mckay in 1992. The algorithm consists of two major parts: the part of extracting the point pairs from the surface data in each coordinate system and the part of deriving the transformation through iterative calculation of distance between pair of points.

The first step of the ICP is data sampling step. The surface registration is a numerical method which required heavy computational cost because that many point pairs are used in iterative computation. Therefore, before extracting the pair of points, both surfaces are sampled to reduce the computational cost. Data sampling in surface

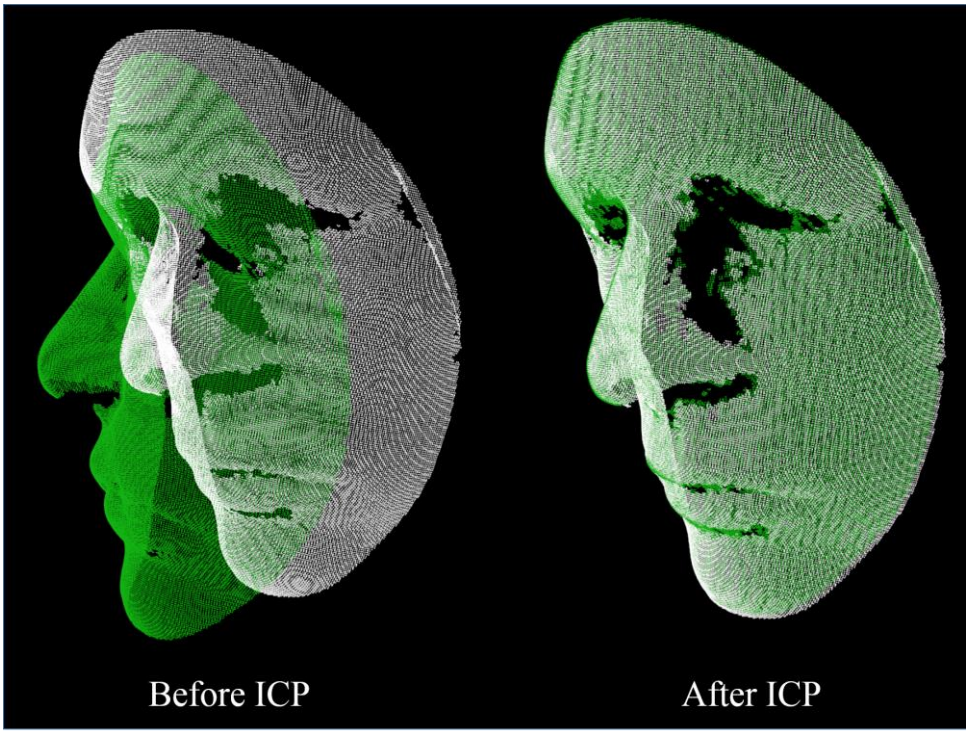

Figure 2.5 Iterative closest point algorithm based surface registration (left) before and (right) after.

registration made use of a strategy to reduce the number of points, while maintain the surface information such as anatomical landmarks, curved feature. Representative sampling methods include the sampling strategy of using all available points, uniform sampling and random sampling.

The next step of the ICP is a point pair matching step. The point pair matching step is a step to search the pair of points in the sampled surface by using the nearest neighbor search method. The nearest neighbor search method is an optimization problem for finding the nearest points. Using the K-dimensional tree (K-d tree) structure, pair of points that match each other on both surfaces are selected.

Among the selected point pairs, incorrectly matched pair of points can be included, and conversely, exactly matched point pairs can be included. The incorrectly matched pair of points are classified as outlier, because it can cause registration error in the registration process. Therefore, inaccurate point pairs are removed by outlier rejection process. On the contrary, exactly matched point pairs are more likely to derive accurate registration result, so the exact point pairs are weighted to calculate more accurate surface registration.

The last step is to continuously derive the transformation through the iterative calculation of distance between point pairs. By applying the derived transformation, the distance between two surface are getting closer in the iterative calculation process. During the distance calculation, when the surface-to-surface distance becomes equal or less than the pre-defined reference distance, the last transformation is derived.

The representative methods for calculating the distance between point pairs are point-to-point metric and point-to-plane metric. The point-to-point metric is the most intuitive method to calculate the Euclidean distance between selected pair of points. The equation point-to-point metric is defined as below:

$$l_i = \sum_i [(\boldsymbol{R}s_i + \boldsymbol{t} - d_i)]^2 \quad (1)$$

where S_i and d_i are the selected points in source surface, and the selected points in target surface, respectively. However, the point-to-point metric may cause registration errors unless the pair of points are exactly matched to each other. The point-to-plane metric is a method of calculating the error that utilizes surface information. The equation of point-to-plane metric is defined as below:

$$l_i = \sum_i [(\boldsymbol{R}s_i + \boldsymbol{t} - d_i) \cdot n_i]^2 \quad (2)$$

where S_i and d_i are the selected points in source surface, and the selected points in target surface, respectively. n_i is the normal vector in target surface. In the point-to-plane error metric, a normal vector of the surface is used for the error calculation. By using the normal vector to calculate the error, more accurate and fast calculation can be performed.

The ICP is an algorithm that derives the transformation between two surfaces through the iterative calculation. The ICP consists of detailed steps of data sampling, point pair matching, outlier rejection, weighting and error calculation. Depending on the purpose of the surface registration, various strategies can be used in detailed steps.

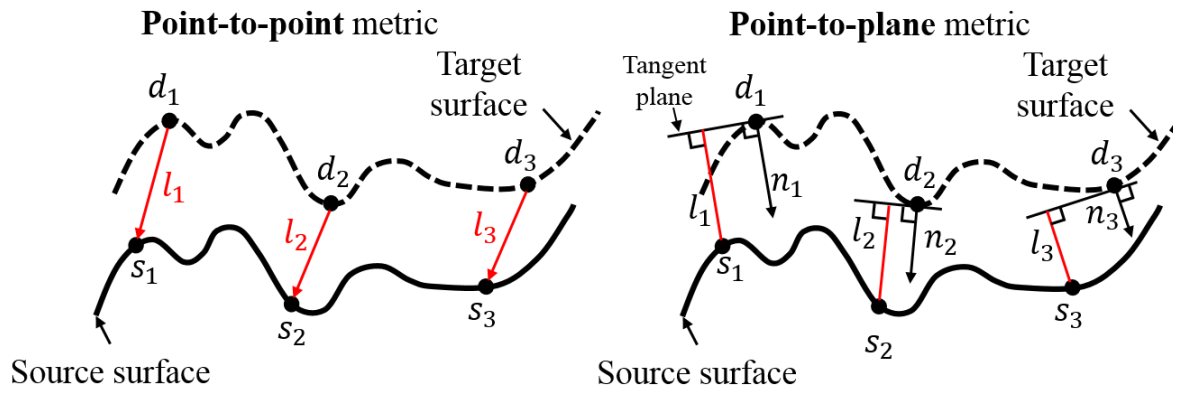

Figure 2.6 Comparison of error metric.

2.3.2 Image-to-patient registration

In the proposed system, the ICP-based surface registration was repetitively performed for the AR visualization. Figure 2.7 shows a pipeline of real-time surface registration.

The reference facial surface data and electrode position data acquired in preparation step are used for surface registration and data visualization. In the ICP algorithm, the previously updated reference facial surface data and the scanned data were used for source data and target data, respectively. As a result of the ICP, the transformation from source to target coordinate system is calculated. Therefore, during the repetitive process, the transformation is updated, which is defined as below:

$$\boldsymbol{T}_{\boldsymbol{A_{i-1}}}^{\boldsymbol{A_i}} \tag{3}$$

where A_i is the current scanning coordinate system, A_{i-1} is the previously updated reference coordinate system and i is index of surface registration which is continuously updated.

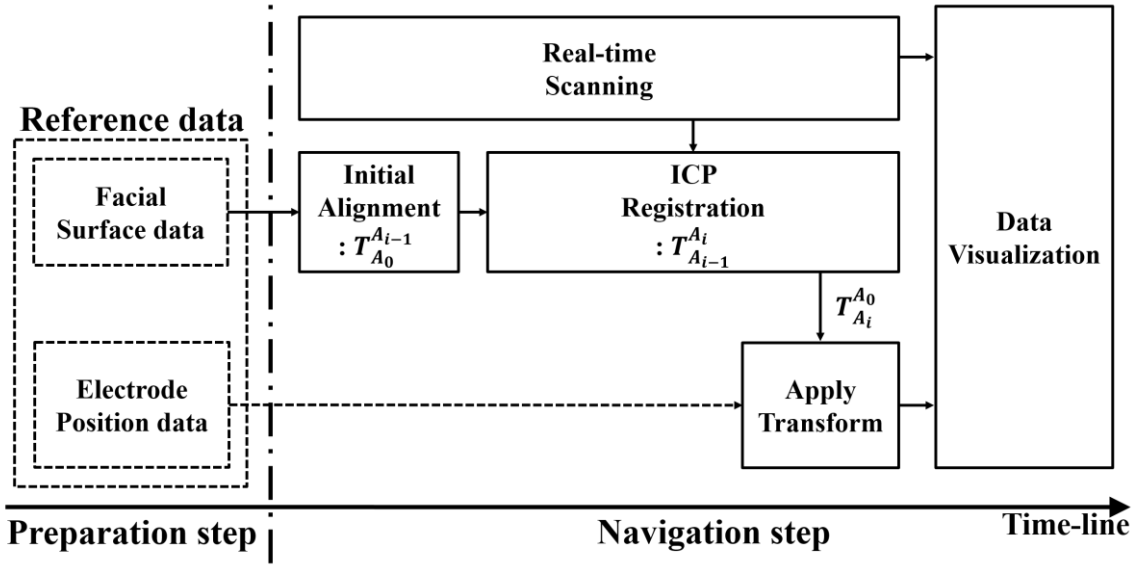

Figure 2.7 Pipeline of real-time surface registration. Based on the parallel process of real-time scanning and ICP registration, the AR data which overlay reference electrode position on to real-time scanning data is visualized.

In the first registration, the ICP between reference facial surface and real-time scanning data is performed with index i = 1 condition. As result of ICP, transformation from reference coordinate system A_0 to current scanning coordinate system A_1 is calculated. Once surface registration is processed, transformation of the previous step is used as initial alignment to update the reference facial surface.

In the proposed registration pipeline, we utilized the transformation of previous step as initial alignment as below:

$$\boldsymbol{T}_{\boldsymbol{A_0}}^{\boldsymbol{A_{i-1}}} \tag{4}$$

where A_0 is the coordinate system of reference data and A_{i-1} is the coordinate system of previously updated scanning data. By applying the prior (i-1) transformation, the reference facial surface data would be closer to current facial surface data before the ICP. The details of initial alignment will be described in section 2.3.3.

As a result of ICP-based surface registration, the transformation from coordinate system of current scanning data to coordinate system of reference data is updated as below:

$$\boldsymbol{T}_{\boldsymbol{A_0}}^{\boldsymbol{A_i}} = \boldsymbol{T}_{\boldsymbol{A_0}}^{\boldsymbol{A_{i-1}}}\, \boldsymbol{T}_{\boldsymbol{A_{i-1}}}^{\boldsymbol{A_i}} \tag{5}$$

By applying the transformation, the reference data is transformed to A_i as shown in Eq. (6):

$$^{\boldsymbol{A_i}}\boldsymbol{\rho} = \boldsymbol{T}_{\boldsymbol{A_0}}^{\boldsymbol{A_i}}\ ^{\boldsymbol{A_0}}\boldsymbol{\rho} \tag{6}$$

where $^{A_i}\rho$ and $^{A_0}\rho$ are the updated reference electrode position data, and the reference electrode position data, respectively.

2.3.3 Adaptive initial alignment

In the ICP-based surface registration, initial guess is important to address the local minimum problem and to reduce the time-taken in case of using two different modalities. The proposed system uses single image modality, the RGB-D camera, and every scanned facial surface data is not significantly different from saved facial surface data in terms of the orientation. In the real-time surface registration pipeline, (i-1) transformation is used for initial alignment in the current (i) registration process. Note that identity matrix was used for the first initial alignment. Once surface registration is processed, transformation of the previous step is used as initial alignment. When constant initial alignment is used, the distance between the source and target data which used for ICP registration is kept constant. However, by using the prior transformation as initial alignment, the source surface would be closer to target data before the ICP registration.

2.3.4 Parallel process for real-time visualization

During the real-time surface registration, ICP algorithm repeatedly processed with about 10,000 corresponding points. To address the heavy computational cost of the ICP, we constructed the system pipeline in parallel as shown in Fig. 2.7. For the parallel processing, we made use of multi thread processing for the real-time scanning, surface registration and data visualization. Consequently, while the ICP processed for surface registration, the real-time scanning data was independently processed for the data visualization.

2.4 Experiment methods

To verify the repeatability of the proposed electrode guidance system, we performed the electrode positioning experiments. The positioning error of proposed system was compared with that of the conventional 10-20 system.

The experimental preparation for the electrode positioning test is shown in Fig. 2.8. A commercial electrode cap with 64 channels (actiCAP, EASYCAP, Herrsching, Germany) was used for electrode positioning, and a head phantom including the human anatomical landmarks was used as a subject. We designated ten target electrodes on an EEG cap to calculate positioning error as shown in Fig. 2.9. The electrodes were denoted by AF3, AF4, FC3, FCz, FC4, CP3, CPz, Cp4, PO3, PO4. To measure the 3D coordinate of electrode position, optical tracking system (OTS) (Polaris vicra, Northern Digital Inc., Waterloo, Canada) was used, which has high tracking accuracy (RMS 0.35 mm) and reliability. To track the electrode position, an OTS marker was attached to the phantom. The electrode positions with respect to the phantom-attached OTS marker were acquired by using hand-held OTS probe.

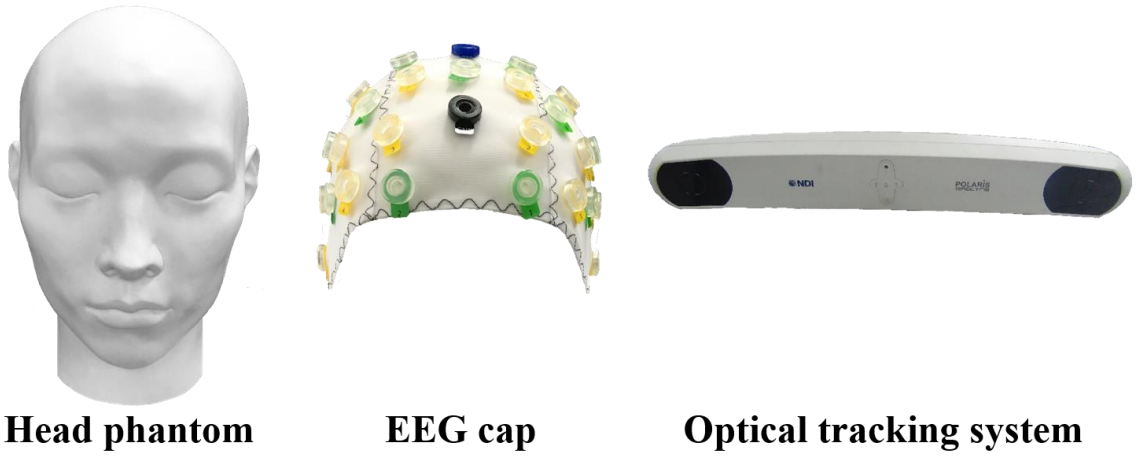

Figure 2.8 Experimental preparation for electrode positioning test.

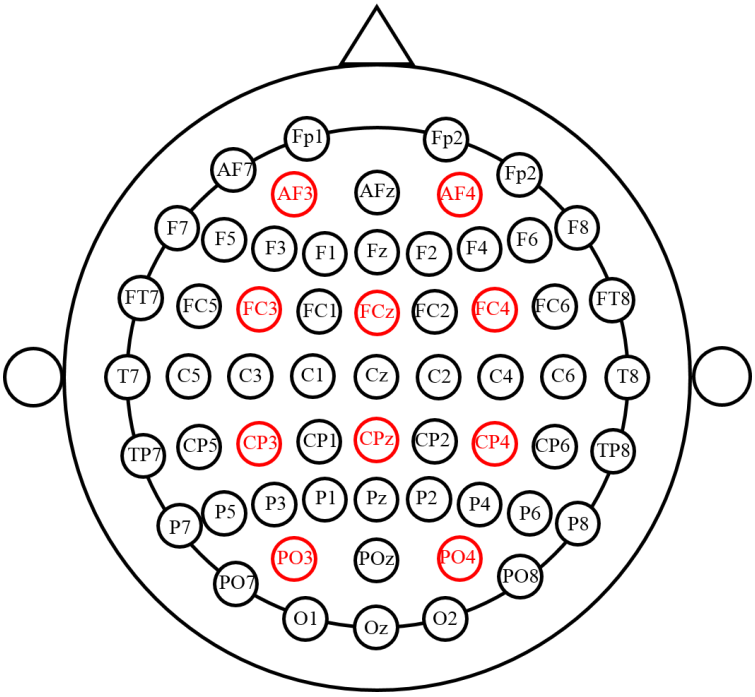

Figure 2.9 Target electrodes (AF3, AF4, FC3, FCz, FC4, CP3, CPz, Cp4, PO3, PO4) to assess the electrode positioning error.

In the experiments, three experimenter participated in this experiment, and placed electrode cap on the phantom. The firstly placed electrode position is used as gold standard. After that, the experimenter repositioned the electrode cap 10 times using the proposed system and 10-20 system, respectively. The experiments were performed over 30 trials for the each of the two systems. To verify the repeatability of electrode position, the positioning error was measured as below:

$$\boldsymbol{Positioning\ error} = \|\boldsymbol{p} - \boldsymbol{p'}\| \tag{7}$$

where p is measured target points after repositioning the electrode in each trial, p' is initially measured points of gold standard.

The optical tracking system (OTS) was used for measuring the electrode position during the experiments. The OTS is a representative system used for real-time position tracking, and it provides tracking accuracy within

0.35mm. During the electrode positioning experiments, the OTS marker was attached on the head phantom in order to measure the position of the electrode with respect to the marker. Then, the position of the electrode is measured based on the phantom-attached marker using the hand-held OTS probe. The position of the phantom-attached marker and the hand-held probe were tracked by OTS as follows:

$$T_{Marker}^{OTS} \tag{8}$$

$$T_{Probe}^{OTS} \tag{9}$$

The position of the placed electrodes can be obtained by calculating the position of the hand-held probe with respect to the phantom-attached marker as shown in Eq. (10):

$$T_{Probe}^{Marker} = T_{OTS}^{Marker}\, T_{Probe}^{OTS} \tag{10}$$

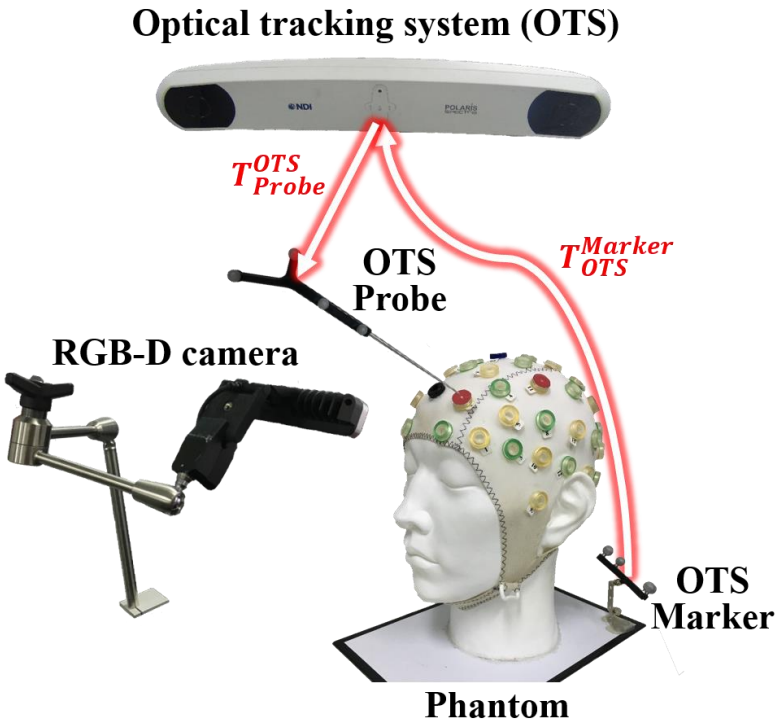

Figure 2.10 Experimental setup for assessing the precision of the electrode positioning.

In the repeatability test, in order to assess the positioning error of the proposed electrode guidance system, the electrode cap was repositioned on the phantom by referring overlaid data. After repositioning the electrode cap, the position of predefined 10 electrodes (AF3, AF4, FC3, FCz, FC4, CP3, CPz, Cp4, PO3, PO4) were again measured to calculate the positioning error. The position of each electrode position was measured by the hand-held OTS probe relative to the phantom-attached OTS marker. The positioning error was calculated using the measured 10 target points and the gold standard points. In order to assess the positioning error of the conventional 10-20 system, the electrode cap was repositioned on the phantom using the international 10-20 system. In the similar way, after repositioning the electrode cap, the predefined 10 target electrodes were measured and the positioning errors were calculated. All repeatability tests were performed under the same experimental condition except the electrodes positioning method.

III. RESULTS

3.1 Evaluation of electrode positioning accuracy

In the phantom study, to validate the repeatability of the electrode positioning, the positioning error was compared the proposed system with conventional 10-20 system. The mean positioning error was 1.8 ± 1.06 mm for the proposed system and 3.24 ± 1.78mm for the 10-20 system as depicted in Table 3.1. According to the literature, in the process of electrode positioning, accuracy less than 5 mm is desirable for dense arrays of electrodes and sophisticated neural source inversion algorithm [16, 17]. When comparing the positioning error of the proposed system with that of the 10-20 system, the proposed system can ensure more stable EEG data according to the neural source inversion algorithm.

Table 3.1. Measured positioning error. (mean ± standard deviation)

	Positioning error (mm)
The proposed system	1.8 ± 1.06
The 10-20 system	3.24 ± 1.78

Table 3.2. Measured positioning error at each target electrodes. (mean ± standard deviation)

Electrode	The proposed system (mm)	The 10-20 system (mm)
AF3	0.9 ± 0.46	2.92 ± 1.86
AF4	1.42 ± 0.67	3.57 ± 2.0
FC3	1.36 ± 0.71	2.82 ± 1.65
FCz	1.41 ± 0.6	3.36 ± 1.69
FC4	2.28 ± 0.87	3.22 ± 1.81
CP3	1.93 ± 0.9	3.41 ± 1.82
CPz	2.03 ± 0.99	3.37 ± 1.34
Cp4	2.25 ± 1.12	2.66 ± 1.69
PO3	2.23 ± 1.32	3.67 ± 1.93
PO4	2.19 ± 1.53	3.37 ± 1.93

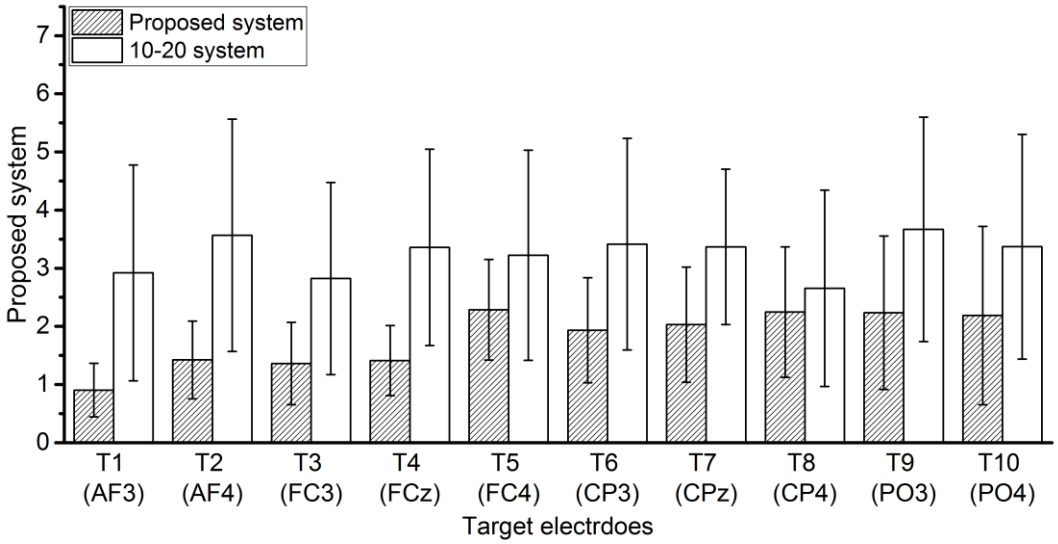

Figure 3.1 Comparison of positioning error at each target electrodes.

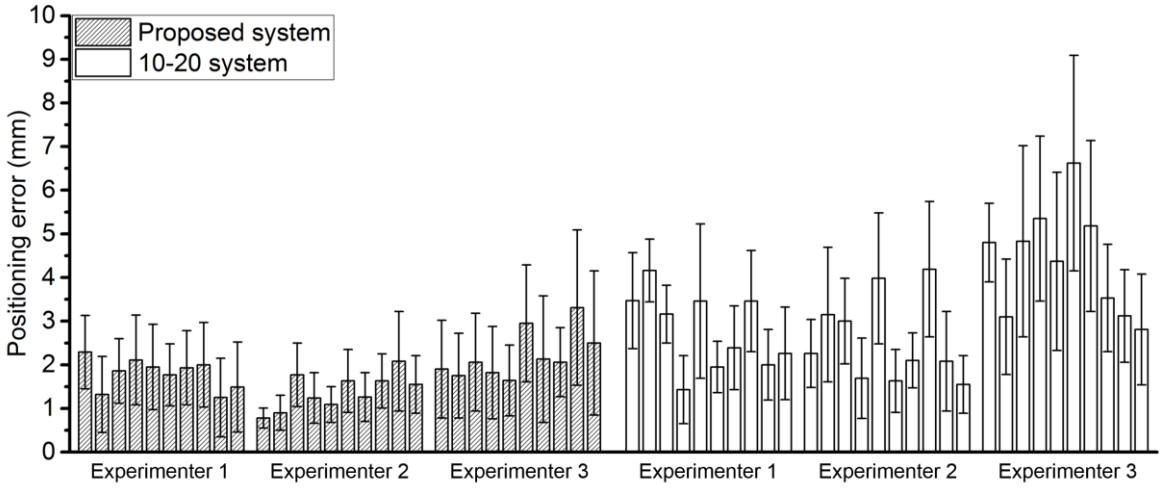

Figure 3.2 Comparison of positioning error among each experimenter.

Compared to the conventional system, both the mean and standard deviation of each positioning error of the proposed system were reduced at all target electrodes. We observed that the positioning error measured at front-located target electrodes, which are AF3, AF4, FC3, and FCz, were smaller than those measured at relatively rear-located target electrodes as shown in Fig. 3.1.

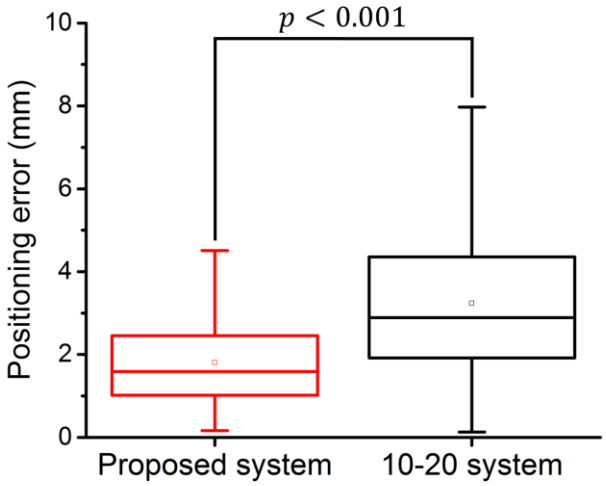

Figure 3.3 Statistical analysis of electrode positioning error.

In the experimental result, there was slight deviation in positioning error among each experimental trial as shown in Fig. 3.2. When analyzing the positioning error for each experimental trial, the deviation of mean positioning error for each trial was 0.54 mm for the proposed system and 1.29 mm for the 10-20 system, respectively.

To assess the statistical significance for improvement of electrode positioning in proposed system, the independent t-test was performed using the OriginLab software (OriginPro 2015, Northampton, Massachusetts, USA) as shown in Fig. 3.3. In the Kolmogorov-Smirnov normality test, at the 0.001 decision level, both experimental results were significantly drawn from a normality distribution population. In the independent t-test, the experimental results show that the proposed system significantly improved the positioning error than the 10-20 system ($p < 0.001$).

3.2 Evaluation of real-time surface registration performance

During the electrode positioning experiments, to assess the performance of the real-time surface registration, the registration error and registration time were measured. The registration error represents the fiducial registration error (FRE) in the process of real-time surface registration. The registration time represents the taken time for one time of registration in the process of the real-time surface registration. The registration error and registration time were measured 50 times from the beginning. The mean registration error was 0.37mm, and the mean registration time was 0.16 seconds as depicted in Table 3.3.

Table 3.3 Performance of real-time surface registration. (mean ± standard deviation)

	The proposed system
Registration error (mm)	0.37 ± 0.05
Registration time (s)	0.16 ± 0.08

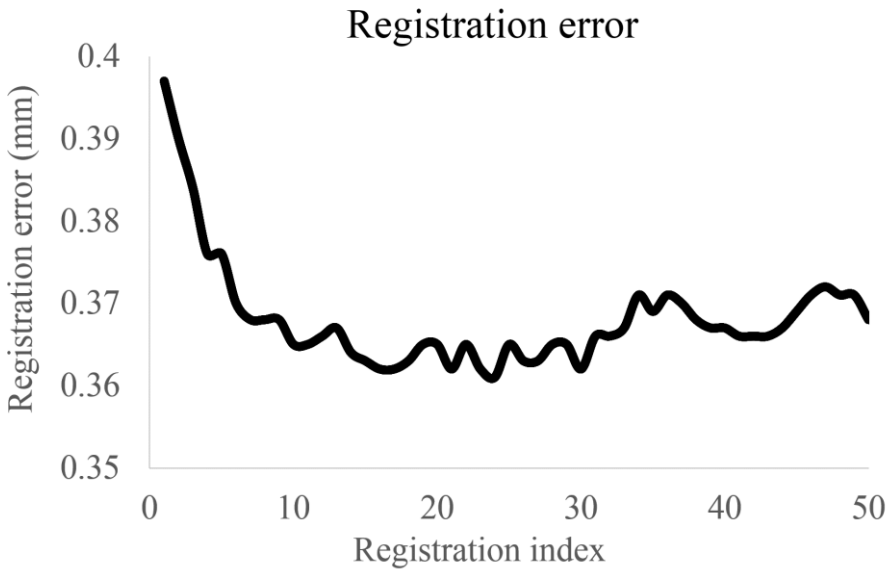

Figure 3.4 Variation of registration error.

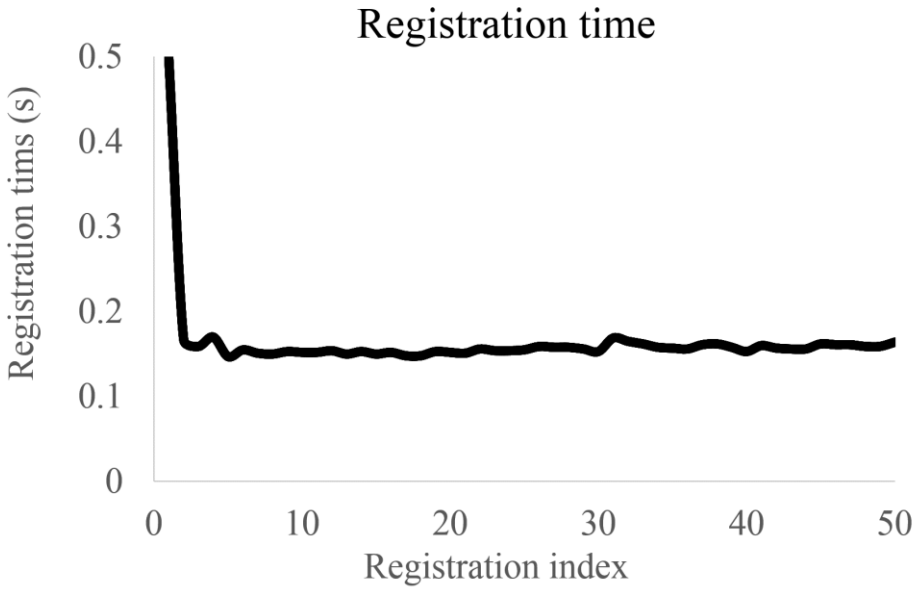

Figure 3.5 Variation of registration time.

The variation of the registration error during the electrode positioning experiments is described in Fig. 3.4. The registration error was decreased at the early stage of registration. After the decreasing, registration error was oscillated at a very small range within 0.1mm, and all registration errors were less than 0.5 mm during the electrode positioning experiments. The variation of registration time during the electrode positioning experiments is described in Fig. 3.5. The registration time was rapidly decreased at the early stage of registration, and then converged to the constant. The average 0.16s of registration time assure the 6.25 frame per second (fps), and the experimental results of electrode positioning showed that 6.25 frame rates was sufficient for AR visualization in the process of electrode guidance.

IV. DISCUSSTION AND CONCLUSION

In this study, we proposed an electrode guidance system based on the markerless AR technique. The proposed system utilized facial surface as reference for AR visualization, thereby no additional manual identification is required in the process of electrode positioning. Thus, because that the human error due to the manual identification does not occur, the positioning precision is improved. The statistical analysis for the results of the phantom study confirmed that the proposed system showed a significant improvement in the positioning error in comparison with that of the conventional 10-20 system ($p < 0.001$).

Experimental result of proposed system showed that both accuracy and precision of the positioning error were improved in target electrodes which are located at the front head compared to that of the target electrodes located at the rear of the head. Due to the narrow field of view (FOV) of the RGB-D camera adopted in this study, a part of electrodes were guided, and the rest of target electrodes were not guided. Despite this limitation, the improvement in the positioning precision by the proposed system was evident from the experimental results, the use of a stereo RGB-D camera still have a possibility to further improve the proposed system in terms of both the positioning accuracy and precision.

When it comes to surface registration, thanks to the parallel pipeline for the surface registration, the real-time scanning data representing the reference electrode locations can be visualized in real time despite the high computational cost of ICP. For the initial alignment of the ICP, we utilized prior transform in iterative registration processes. Due to the use of (i-1) transformation as a starting value in the current (i) registration process, computational time for registration was efficiently saved. Throughout the experiments, the ICP surface registration was performed with fixed parameter conditions including the point-to-point error metric and uniform data sampling; the registration accuracy and the resultant positioning precision according to different parameter

conditions should be further investigated.

Compared with the previous approaches [4, 5], the proposed system only used an inexpensive RGB-D camera to perform the electrode guidance system with the precision. Using only one RGB-D camera was cost-effective and made it simple to configure the proposed system. On the other hand, the performance of the proposed system is highly dependent on the performance of RGB-D camera. However, the limitation of the RGB-D camera would be improved by using the stereo camera. The proposed system can be used not only for EEG electrode guidance but also for the other application for AR visualization.

V. REFERENCE

[1] S. R. Atcherson, H. J. Gould, M. A. Pousson, and T. M. Prout, "Variability of electrode positions using electrode caps," *Brain Topography,* vol. 20, pp. 105-111, Win 2007.

[2] P. Giacometti and S. G. Diamond, "Compliant head probe for positioning electroencephalography electrodes and near-infrared spectroscopy optodes," *J Biomed Opt,* vol. 18, p. 27005, Feb 2013.

[3] T. D. Lagerlund, F. W. Sharbrough, C. R. Jack, B. J. Erickson, D. C. Strelow, K. M. Cicora*, et al.*, "Determination of 10–20 system electrode locations using magnetic resonance image scanning with markers," *Electroencephalography and clinical neurophysiology,* vol. 86, pp. 7-14, 1993.

[4] P. He and J. R. Estepp, "A practical method for quickly determining electrode positions in high-density EEG studies," *Neurosci Lett,* vol. 541, pp. 73-6, Apr 29 2013.

[5] P. Giacometti, K. L. Perdue, and S. G. Diamond, "Algorithm to find high density EEG scalp coordinates and analysis of their correspondence to structural and functional regions of the brain," *Journal of Neuroscience Methods,* vol. 229, pp. 84-96, May 30 2014.

[6] V. Jurcak, D. Tsuzuki, and I. Dan, "10/20, 10/10, and 10/5 systems revisited: their validity as relative head-surface-based positioning systems," *Neuroimage,* vol. 34, pp. 1600-1611, 2007.

[7] H. H. Jasper, "The ten twenty electrode system of the international federation," *Electroencephalography and clinical neurophysiology,* vol. 10, pp. 371-375, 1958.

[8] J. F. Echallier, F. Perrin, and J. Pernier, "Computer-assisted placement of electrodes on the human head," *Electroencephalogr Clin Neurophysiol,* vol. 82, pp. 160-3, Feb 1992.

[9] L. Koessler, L. Maillard, A. Benhadid, J. P. Vignal, M. Braun, and H. Vespignani, "Spatial localization of EEG electrodes," *Neurophysiol Clin,* vol. 37, pp. 97-102, Apr-May 2007.

[10] J.-D. Lee, C.-H. Huang, T.-C. Huang, H.-Y. Hsieh, and S.-T. Lee, "Medical augment reality using a markerless registration framework," *Expert Systems with Applications,* vol. 39, pp. 5286-5294, 2012.

[11] M. C. de Farias Macedo and A. L. A. Junior, "Improving on-patient medical data visualization in a markerless augmented reality environment by volume clipping," in *2014 27th SIBGRAPI Conference on Graphics, Patterns and Images*, 2014, pp. 149-156.

[12] N. Mahmoud, Ó. G. Grasa, S. A. Nicolau, C. Doignon, L. Soler, J. Marescaux*, et al.*, "On-patient see-through augmented reality based on visual SLAM," *International Journal of Computer Assisted Radiology and Surgery,* pp. 1-11, 2016.

[13] R. B. Rusu and S. Cousins, "3d is here: Point cloud library (pcl)," in *Robotics and Automation (ICRA), 2011 IEEE International Conference on*, 2011, pp. 1-4.

[14] J. Salvi, C. Matabosch, D. Fofi, and J. Forest, "A review of recent range image registration methods with accuracy evaluation," *Image and Vision computing,* vol. 25, pp. 578-596, 2007.

[15] P. J. Besl and N. D. McKay, "Method for registration of 3-D shapes," in *Robotics-DL tentative*, 1992, pp. 586-606.

[16] B. H. Brinkmann, T. J. O'Brien, M. A. Dresner, T. D. Lagerlund, F. W. Sharbrough, and R. A. Robb, "Scalp-recorded EEG localization in MRI volume data," *Brain Topogr,* vol. 10, pp. 245-53, Summer 1998.

[17] L. Koessler, A. Benhadid, L. Maillard, J. P. Vignal, J. Felblinger, H. Vespignani*, et al.*, "Automatic localization and labeling of EEG sensors (ALLES) in MRI volume," *Neuroimage,* vol. 41, pp. 914-923, 2008.

[18] T. Gasser, P. Bächer, and H. Steinberg, "Test-retest reliability of spectral parameters of the EEG," *Electroencephalography and clinical neurophysiology,* vol. 60, pp. 312-319, 1985.

요 약 문

실시간 표면 정합 기반 전극배치 유도 시스템

뇌전도(Electroencephalography, EEG)는 대표적인 비침습적 뇌 활동 측정 방법으로, 전기적 신호를 바탕으로 뇌 활동을 측정한다. EEG 를 사용하는 중·장기적 연구에서는 반복 측정의 신뢰성(Test-retest reliability)을 보장하기 위해서 재현성 있는 전극 배치가 중요하다. 10-20 시스템은 재현성 있는 전극 배치를 위해 개발된 대표적인 전극 배치 시스템이다. 기존의 10-20 시스템은 비근점, 뒤통수점, 좌-우 이개전방점과 같은 인체의 해부학적 특징점을 바탕으로 전극을 배치하게 된다. 하지만 해부학적 특징점은 환자에 따라 변동이 크고 불분명하며, 시각과 촉각에 의존하여 특징점을 인식하고 위치를 측정해야 하므로 오차의 발생 가능성이 크다. 상기 문제점을 해결하기 위해서 본 연구에서는 마커리스 증강현실 기술을 활용하여 보다 정확한 전극배치가 가능한 시스템을 제안하였다. 제안하는 시스템은 RGB-D 카메라만으로 구성되어 비용 효율이 높고, 증강현실의 영상 정보를 바탕으로 간편하고 정확한 전극의 배치를 돕는다. EEG 전극배치를 위한 영상정보를 제공하기 위해서, RGB-D 카메라의 실시간 스캔 정보와 저장된 기준 정보간의 실시간 표면을 진행한다. 실시간 표면 정합 결과, 얼굴 표면 정보를 기준으로 저장된 기준 전극위치와 실시간 전극위치가 함께 시각화 되고, 영상 정보를 바탕으로 실시간 전극 위치를 기준 전극 위치에 중첩하여 위치시킴으로써 재현성 있는 전극 배치가 가능하다. 제안하는 시스템은 전극배치 과정에서 별도의 해부학적 특징점 인식이 필요하지 않으므로 간편하고 정확한 전극배치를 보장할 수 있다. 제안하는 시스템의 평가를 위하여, 기존의 10-20 시스템과 전극 배치오차 비교 실험을 진행하였다. 해부학적 특징점이 표현된 두상모형을 사용하여 실험을 진행하였으며, 제안하는 시스템과 기존의 10-20 시스템을 사용하여 각각 20 회 전극 배치오차를 측정하였다. 실험결과, 제안하는 시스템의 평균 배치오차가 기존의 시스템에 비해 크게 감소함을 확인하였다. 따라서, 제안하는 시스템은 EEG 를 사용하는 중·장기적 연구에서 간편하고 재현성 있는 전극배치를 제공할 것으로 기대한다.

핵심어: 전극배치 시스템, 10-20 시스템, 마커리스 증강현실, 표면 정합.

APPENDIX A

Results using 10-20 System										
	T1 (AF3)	**T2 (AF4)**	**T3 (FC3)**	**T4 (FCz)**	**T5 (FC4)**	**T6 (CP3)**	**T7 (CPz)**	**T8 (CP4)**	**T9 (PO3)**	**T10 (PO4)**
1	4.309945	1.923026	3.775525	3.246189	1.490434	4.205691	4.341666	2.730576	3.907243	4.743089
2	4.454187	5.093385	2.839735	5.093716	3.785506	3.285322	4.300778	3.94951	4.424958	4.416393
3	3.92043	4.139474	2.820455	4.196562	3.013807	2.530862	2.991322	2.633	2.75499	2.633576
4	1.48428	2.902709	1.298588	2.406382	2.048126	0.994696	1.023672	0.60518	0.619405	0.911461
5	5.226402	4.652521	5.149172	5.083069	2.832204	4.071988	3.029585	0.882604	3.473816	0.193956
6	0.953497	1.799189	2.388689	1.020631	1.835219	2.705218	2.123451	1.9258	2.497903	2.28404
7	0.518758	1.374651	2.067689	2.392431	2.049717	3.623105	3.128366	2.747867	3.518521	2.458431
8	4.264525	3.373064	3.516133	4.627984	1.278632	4.272324	3.034087	2.100518	5.023124	3.100258
9	1.478618	0.53932	1.315597	2.344081	1.646972	2.170849	2.811412	2.092728	3.411414	2.180507
10	0.364116	1.520098	1.286203	2.030894	1.584206	2.819059	3.407334	2.988293	3.606743	3.032673
11	3.920005	2.384963	1.999103	2.67951	2.627316	2.600027	1.917934	1.084045	1.926102	1.488064
12	3.612595	4.217645	2.54567	3.072024	6.050673	0.530389	2.275115	4.025256	1.538021	3.67333
13	1.71239	1.118125	2.959408	2.505431	3.504734	4.112558	4.254882	3.245599	3.328164	3.218571
14	1.48907	3.180447	0.126897	1.614776	3.039496	1.762894	1.996388	1.374374	1.524034	0.781572
15	5.048244	4.021753	2.897475	3.837159	4.640889	1.318435	3.285923	5.446308	2.819236	6.493147
16	1.232036	2.269143	0.899458	1.867968	2.388288	0.231433	1.62324	2.611564	1.76726	1.396879
17	2.348999	1.728556	2.740604	1.773653	1.430098	2.840152	2.122967	0.907804	2.558857	2.535419
18	4.038621	4.752736	4.098086	4.43363	6.941394	2.821433	3.04734	5.477553	1.308412	4.951207
19	0.618476	1.692354	1.16192	1.911551	1.30826	2.786317	2.77347	1.761957	4.700994	2.095907
20	1.478822	1.545411	1.516366	2.200617	0.795804	2.50472	2.43911	0.553692	1.2141	1.214394
21	3.263021	5.582596	4.037989	5.42718	4.994756	4.963319	4.843814	3.693668	6.246331	4.965637
22	0.144448	4.219054	2.512644	3.066273	4.36621	3.915601	4.109144	4.057566	2.390433	2.237544
23	4.485734	6.737868	4.852887	4.781244	2.254488	6.093863	4.627745	0.3267	7.740477	6.418446
24	4.36943	5.171395	1.367815	4.505764	6.845725	3.751884	6.763871	7.393627	6.694164	6.674912
25	2.495729	6.91389	3.703618	5.496601	6.890442	4.851177	5.561519	4.719875	2.41474	0.656526
26	7.960557	8.799069	7.975353	8.146669	5.364007	8.886398	5.962331	0.628408	6.846467	5.618298
27	4.896707	6.43936	5.992786	5.788317	2.685968	6.980179	4.312611	1.178162	7.248664	6.304393
28	4.000404	3.30715	2.630796	1.126034	3.05293	4.54024	3.013023	3.42592	5.511444	4.692782
29	1.949531	2.686464	2.654962	2.677961	1.790769	3.487306	3.848451	2.654116	4.262541	5.152572
30	1.553925	2.886245	1.562015	1.423266	4.16028	2.750345	2.037026	2.432467	4.745801	4.597768

Results using Proposed System										
	T1 (AF3)	**T2 (AF4)**	**T3 (FC3)**	**T4 (FCz)**	**T5 (FC4)**	**T6 (CP3)**	**T7 (CPz)**	**T8 (CP4)**	**T9 (PO3)**	**T10 (PO4)**
1	0.521522	1.532631	2.475428	2.798694	2.863675	2.75578	2.801637	2.911618	2.841531	1.393236
2	0.522688	1.171019	0.627749	0.664913	3.322817	2.248101	0.845706	1.044663	1.642704	1.151169
3	0.851513	1.310378	2.025622	1.556236	3.115904	2.010309	1.910568	2.9735	1.097835	1.70423
4	1.362428	0.207095	2.450967	2.041451	2.901343	2.77786	2.314736	3.906522	1.155301	1.984284
5	1.037763	1.20581	1.030903	1.815914	2.619405	2.371296	1.582669	2.504715	4.118077	1.172967
6	0.253572	1.791295	2.338382	1.334908	2.652834	2.032425	1.95606	2.450445	1.186015	1.741506
7	0.646455	1.824882	2.089453	1.910137	2.863701	2.841666	1.705606	3.215906	1.233226	0.95686
8	0.817207	1.366295	2.556139	1.328122	1.894364	2.824221	1.865835	3.972927	0.936246	2.460998
9	0.228833	2.940116	1.018966	1.017632	1.755131	1.052587	1.051809	2.527288	0.431373	0.463379
10	0.219831	2.752221	1.415347	0.737916	2.164372	2.068503	1.064709	3.181879	1.155599	0.164246
11	0.660814	0.973655	0.36336	1.13909	0.871143	0.809285	0.677025	0.945576	0.789531	0.546162
12	1.558699	1.293624	0.637941	1.04789	1.331877	0.348595	0.626502	0.836817	0.434088	0.879988
13	2.135388	2.86357	1.328096	2.088215	2.438422	0.434845	1.672442	1.947511	0.808227	1.968909
14	0.630023	1.572511	0.428622	1.610597	1.753371	1.069046	1.811502	0.945531	1.990563	0.585102
15	1.797286	1.634313	0.615567	1.278751	1.165882	0.606778	0.7833	0.945897	1.272421	0.789574
16	1.232036	2.269143	0.899458	1.867968	2.388288	0.231433	1.62324	2.611564	1.76726	1.396879
17	0.961287	1.611508	0.575754	1.116793	1.528186	2.025726	1.108798	0.459006	2.119273	1.072175
18	0.834475	1.255817	1.387499	1.307447	1.052809	2.079075	2.036999	1.956393	2.916367	1.522866
19	0.618476	1.692354	1.16192	1.911551	1.30826	2.786317	2.77347	1.761957	4.700994	2.095907
20	1.478822	1.545411	1.516366	2.200617	0.795804	2.50472	2.43911	0.553692	1.2141	1.214394
21	1.243704	0.409707	1.420007	0.817479	1.597925	1.216571	2.316321	3.139819	3.055324	3.788357
22	1.01232	1.047851	0.926529	0.89526	2.720296	1.61873	2.1001	1.087059	2.322165	3.808597
23	0.901813	1.767368	0.609308	0.891048	3.099388	1.387738	3.228074	2.038427	3.251882	3.4699
24	0.56554	0.833282	0.776795	0.904821	2.769269	1.434147	2.039022	2.334519	3.170517	3.403866
25	1.13895	1.634403	1.545423	0.428696	1.327094	2.082683	1.248296	1.146041	3.220694	2.59808
26	0.965277	1.070836	2.378618	2.202111	3.774095	3.491104	3.808652	3.930415	2.706299	5.214511
27	0.337286	0.629734	1.081633	0.5546	2.247174	2.616105	2.887031	2.554733	4.508228	3.908062
28	1.175762	1.222955	2.305726	1.090125	3.210755	2.637504	2.309742	1.535553	2.007343	3.137843
29	0.827601	0.735205	2.133814	2.484442	3.544311	3.489511	5.089849	3.865904	4.815932	6.121573
30	0.570796	0.524179	0.725394	1.302113	3.444514	2.136407	3.209508	4.071828	4.169831	4.877329